

An Assessment of Generating Quasi-Static Magnetic Fields Using Laser-Driven “Capacitor” Coils

J. L. Peebles, J. R. Davies, D. H. Barnak, F. Garcia-Rubio, P. V. Heuer, G. Brent, R. Spielman, and R. Betti

Laboratory for Laser Energetics, University of Rochester

Over the previous decade, numerous experiments have been performed using a laser to drive a strong, quasi-static magnetic field. Field strength and energy density measurements of these experiments have varied by many orders of magnitude, painting a confusing picture of the effectiveness of these laser-driven coils (LDC’s) as tools for generating consistent fields. At the higher end of the field energy spectrum, kilotesla field measurements have been used to justify future experimental platforms, theoretical work, and inertial confinement fusion concepts. In this work we present the results from our own experiments designed to measure magnetic fields from LDC’s as well as a review of the body of experiments that have been undertaken in this field. We demonstrate how problems with prior diagnostic analyses have led to overestimates of the magnetic fields generated from LDC’s.

The first aspect of these experiments that must be addressed is conversion of laser energy to magnetic-field energy. While it is easy to claim results are feasible as long as energy in the magnetic field is less than the energy in the driving laser, the reality is that no laser experiment has a significant amount of free energy to generate a magnetic field. For certain experiments, the total laser absorption can be as high as 90%, but for the majority of experiments using drivers similar to those in most LDC experiments, it is much lower (50%). Hot-electron production is a potential source of free energy. Up to ~30% of the laser energy could be converted to hot electrons at the higher values of $I\lambda^2$ used.¹ For the parameters of most LDC experiments with lower $I\lambda^2$, however, a smaller percentage of the laser energy would be converted into hot electrons.² When considering that all the potential energy sinks for this conversion, at most half the energy put into hot electrons can be converted to current. Therefore, a physically reasonable upper limit on laser-energy conversion to magnetic energy would appear to be 15% and, in most cases, should be much less. Examining each LDC experiment’s energy conversion by integrating the field energy density ($B^2/2\mu_0$) over a $10 \times 10 \times 10\text{-mm}^3$ volume produces the results in Fig. 1.^{3–15}

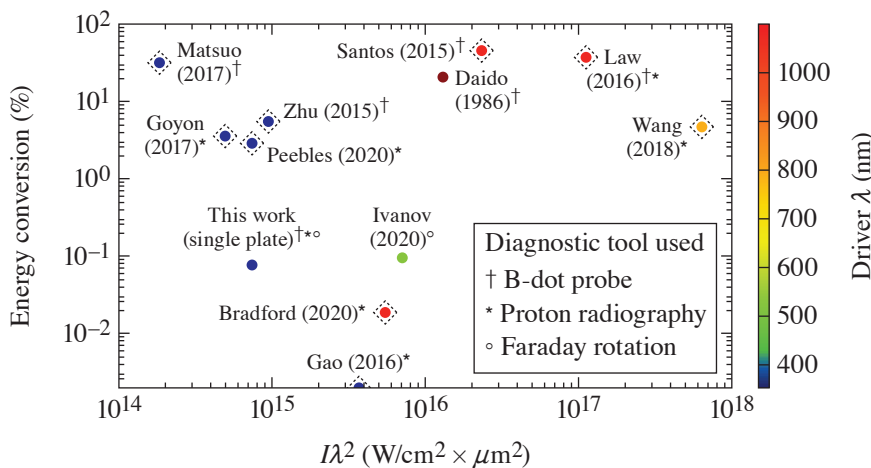


Figure 1
The calculated energy conversion from laser energy to field energy for the variety of LDC experiments.^{3–15} Superscripts denote the diagnostic tool used to arrive at the result, while dotted diamonds around a shot indicate the presence of a short-pulse beam on the experiment. Experiments with conversion over 10% stand out because they have suspiciously high energy conversion.

E30081JR

Looking at the body of experiments, a trend emerges: several experiments measured fields that contained energy equal to 30%–40% of the energy of the driving laser. These experiments also coincidentally measured the primary result using the B-dot while a short-pulse, high-intensity laser was present. This is highly indicative that the B-dot probe responds differently to these experiments than other diagnostics. To address this, we performed our own experiments with LDC's using the entire battery of magnetic-field diagnostics: axial and transverse proton probing, Faraday rotation, and B-dot probes, as shown in Fig. 2. Two types of coils were tested to examine the effect of having the second plate on the target and were driven by a 1-ns, up-to-1.25-kJ, long-pulse UV beam.

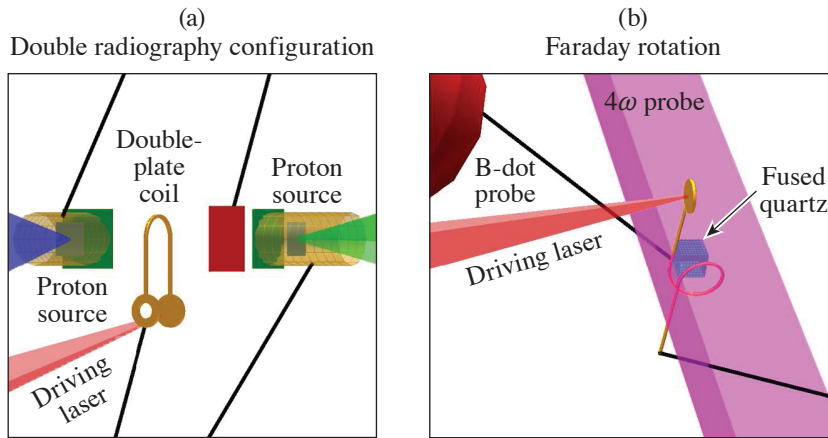
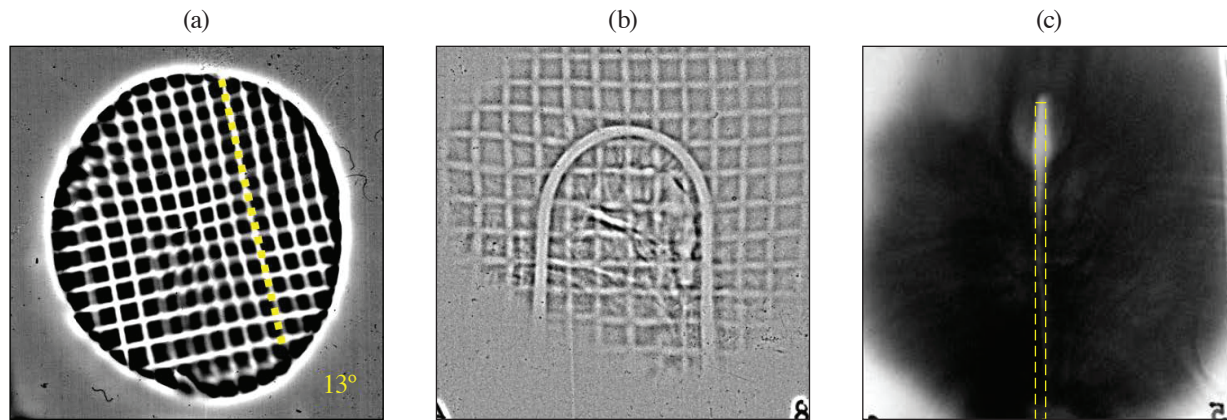


Figure 2
Experimental platform used to study the fields generated by LDC targets using a battery of diagnostics. (a) One campaign used both the sidelighter and backlighter beams to simultaneously probe the coil transverse and axially with protons. (b) A setup used the 4ω probe with a piece of fused quartz for Faraday rotation (polarimetry). All experiments had a B-dot probe placed roughly 2 cm from the loop attached to a 6-GHz-bandwidth balun and scope.

E30069JR

Several results from our experiments are shown in Fig. 3. A 40-T reference magnetic field was generated by MIFEDS (magneto-inertial fusion electrical discharge system) and probed by the axial proton probe [Fig. 3(a)]. As protons travel through the magnetic field, a secondary deflection from the radial magnetic field induces a rotation of the reference mesh. This rotation increases with field strength and decreases with proton energy. The same proton probe was applied to our LDC's and produced no measurable rotation. This indicates that the magnetic field in the LDC is below the measurement threshold (20 kA in the coil) for the axial probe. Using the more-sensitive transverse proton probe on the LDC produces a bulge near the top of the LDC, indicative of a small current of 2.5 kA. This current is far below that measured by most of the experiments shown in Fig. 1 and indicates a much poorer laser-to-field-energy conversion ratio.



E30080JR

Figure 3
Axial proton probes of a known magnetic field generated by (a) MIFEDS and (b) a double-plate LDC. In (a) MIFEDS generated a 40-T field that induced an apparent rotation of the mesh fiducial dependent on the proton energy. This diagnostic technique is sensitive to fields generated by currents greater than 20 kA. In (b) no such rotation is measured, indicating that any current must be less than 20 kA. (c) A transverse proton probe of the same LDC shows a slight bulge near the top of the coil, indicating a current of ~2.5 kA.

Supplementing the proton radiography measurements were the Faraday rotation and B-dot probe diagnostics. Faraday rotation measures the magnetic field in a medium by comparing the rotation difference between orthogonal polarizations as they pass through the medium in the presence of a magnetic field. In the case of our LDC experiment, no significant rotation was measured in the two polarizations of the 4ω probe. The error in the measurement between the two polarizations is $\pm 2\%$, which corresponds to a measurement limit of a 7.5-kA current in our coil, consistent with a 2.5-kA measurement of the proton probe. The B-dot probe acquired measurements in all experimental configurations, both with and without the short-pulse beams. When comparing the data in Fig. 4 it is clear that the B-dot probe is heavily influenced by the presence of the short-pulse beam. Since the short pulse-beams were timed 1 ns after the long-pulse drive beam in order to probe the interaction after the drive, the signal contributions between the two types of beams can be differentiated on the scope. When we account for the scope and cable attenuation based on assumed signal frequency, the signal from the long-pulse beam implies a current of 62.5 kA, much higher than all other diagnostics. The signal from the short pulse is roughly an order of magnitude higher than that of the long pulse, implying a very unrealistic current of over 600 kA.

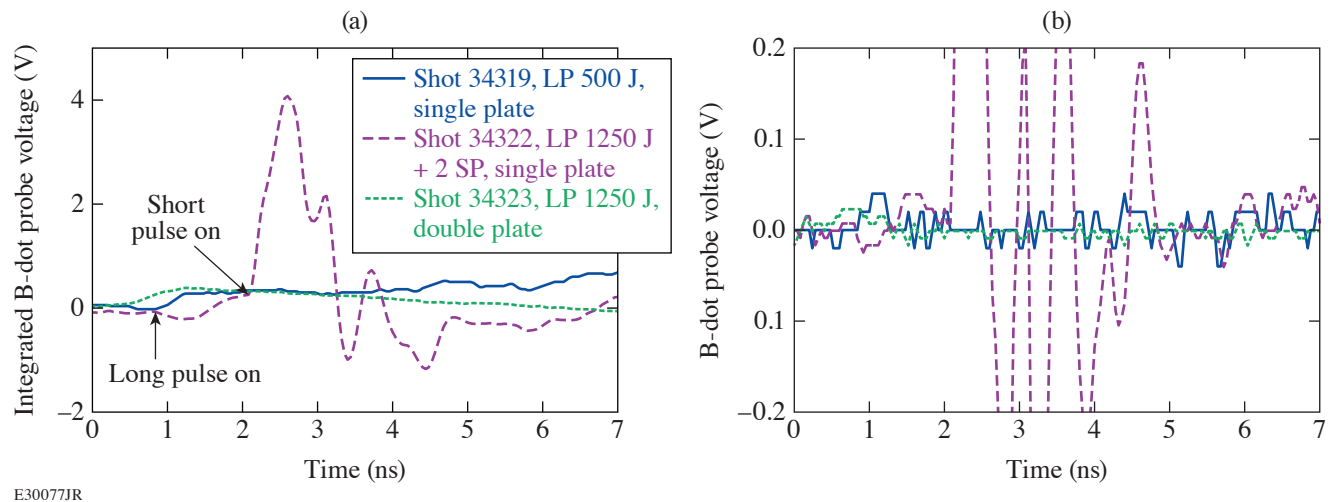


Figure 4

(a) Integrated B-dot probe signals for three different shots: two without short-pulse beams with different coil types and one with the short-pulse beams. The signal with the short-pulse beams is over $10\times$ higher (4 V compared to 0.34 V) than that of the long-pulse beam drive only. The spike in signal from the short pulse is delayed compared to the long pulse due to the beam timings used on the experiment and time of flight from target to B-dot probe. (b) Raw data for the same shots, demonstrating the poor signal-to-noise ratio on the experiments without the short pulse. The signal is varying as quickly as the diagnostic can measure, indicating that the majority of signal is oscillating faster than 6 GHz.

While a B-dot probe (with differentiation) is designed in theory to measure only a changing magnetic field, in reality the entire probe and cabling is subject to effects that are not completely neutralized, such as capacitive coupling, where electric fields can induce significant voltage. The signal generated on the B-dot probe by the short-pulse beam clearly indicates current that is unphysical from a conservation of energy perspective; however, this effect explains the conclusions of many previous LDC experiments shown in Fig. 1. The “highest performing” experiments also utilized a B-dot probe in conjunction with proton radiography using a short-pulse, high-intensity beam. Similar to our experiment, other diagnostics (proton radiography or Faraday rotation) typically indicated field values far lower than the B-dot probe; however, in most of these experiments the B-dot probe result is given preference because of its larger value, despite the poorer accuracy of the method. When we account for this short-pulse interference of the B-dot probe, the majority of results fall into more-reasonable energy conversion ratios of, at most, a few percent.

We began experiments on laser-driven coils to develop a consistent platform for applying and measuring external magnetization of an experiment. In some regards we were successful: a field was measured that was relatively consistent across all diagnostics; however, the field values we measured departed severely from those in other publications. These experiments comprehensively demonstrated that laser-driven coils are not well described by a circuit or capacitor model nor do they produce

uniform consistent fields. Our experiments at best could convert less than a percent of driving laser energy into the magnetic field at the coil, far less than the optimistic conclusions of other experiments. B-dot probes and Faraday rotation were found to be ineffective at measuring magnetic fields in our higher-power LDC experiments because they were subject to the extreme radiation and electric-field environment. Proton radiography produced a precise and detailed picture of electrostatic and magnetic fields around the LDC, but a higher degree of confidence in our conclusions drawn from radiographs was obtained only by probing in two directions simultaneously.

This material is based upon work supported by the Department of Energy National Nuclear Security Administration under Award Numbers DE-NA0003856 and DE-NA0003868, the Office of Fusion Energy Sciences Award Number DE-SC0021072, the University of Rochester, and the New York State Energy Research and Development Authority.

1. J. R. Davies, *Plasma Phys. Control. Fusion* **51**, 014006 (2009).
2. C. Garban-Labaune *et al.*, *Phys. Rev. Lett.* **48**, 1018 (1982).
3. H. Daido *et al.*, *Phys. Rev. Lett.* **56**, 846 (1986).
4. J. J. Santos *et al.*, *New J. Phys.* **17**, 083051 (2015).
5. K. F. F. Law *et al.*, *Appl. Phys. Lett.* **108**, 091104 (2016).
6. C. Courtois *et al.*, *J. Appl. Phys.* **98**, 054913 (2005).
7. A. Tarifeño, C. Pavez, and L. Soto, *J. Phys.: Conf. Ser.* **134**, 012048 (2008).
8. L. Gao *et al.*, *Phys. Plasmas* **23**, 043106 (2016).
9. C. Goyon *et al.*, *Phys. Rev. E* **95**, 033208 (2017).
10. W. Wang *et al.*, *Phys. Plasmas* **25**, 083111 (2018).
11. B. J. Zhu *et al.*, *Appl. Phys. Lett.* **107**, 261903 (2015).
12. K. Matsuo *et al.*, *Phys. Rev. E* **95**, 053204 (2017).
13. V. V. Ivanov *et al.*, *Phys. Plasmas* **27**, 033102 (2020).
14. P. Bradford *et al.*, *High Power Laser Sci. Eng.* **8**, e11 (2020).
15. J. L. Peebles *et al.*, *Phys. Plasmas* **27**, 063109 (2020).